Retrograde endocannabinoid regulation of GABAergic inhibition in the rat dentate gyrus granule cell

Masako Isokawa and Bradley E. Alger

Department of Physiology and Program in Neuroscience, University of Maryland School of Medicine, 655 W. Baltimore Street, Baltimore, MD 21201, USA

The dentate gyrus is a key input gateway for the hippocampus, and dentate function is potently regulated by GABAergic inhibition. GABAergic inhibition is plastic and modulated by many factors. Cytoplasmic calcium ($[Ca^+]_i$) is one of these factors, and its elevation inhibits GABA-mediated transmission in the hippocampus including the dentate gyrus granule cells (DGCs). We examined whether the $[Ca^+]_i$-dependent decrease of $GABA_A$ receptor-mediated inhibitory postsynaptic current (IPSC) is explained by the retrograde suppression of GABA release caused by the depolarization-induced elevation of $[Ca^+]_i$ in DGCs (DSI: depolarization-induced suppression of inhibition). Repeated brief depolarizations or a single long depolarization inhibited spontaneous IPSCs with amplitudes over 25 pA for up to a minute, and reduced the amplitude of IPSCs evoked by direct stimulation in the molecular layer, suggesting that DGCs are susceptible to DSI. The magnitude of DSI correlated linearly with the duration of depolarization, and so did the increase of $[Ca^+]_i$. DSI was blocked by intrapipette application of BAPTA. In addition, bath application of thapsigargin and ryanodine, and intrapipette application of ryanodine and ruthenium red reduced the $[Ca^+]_i$ increase caused by the DSI-inducing depolarization, and substantially reduced the magnitude of DSI. Finally, the cannabinoid receptor agonists, CP55,942 and WIN55,212-2, mimicked DSI and prevented further IPSC reduction by DSI. DSI was blocked by the antagonist, SR141716A. We conclude that GABAergic inhibition in DGCs is subject to endogenous cannabinoid (eCB)-mediated retrograde regulation, and this process involves a depolarization-initiated release of Ca^+ from ryanodine-sensitive stores. Our findings suggest eCBs probably have physiological functions in the regulation of GABAergic plasticity in the dentate gyrus.

(Resubmitted 6 July 2005; accepted after revision 18 July 2005; first published online 21 July 2005)
Corresponding author M. Isokawa: Department of Biological Sciences, University of Texas at Brownsville, 80 Fort Brown, Brownsville, TX 78520, USA. Email: misok001@yahoo.com

GABAergic inhibition exerts a powerful synaptic control over neuronal excitability. Slight changes in GABAergic inhibition influence excitatory transmission and the induction of various forms of synaptic plasticity, directly and indirectly. Indeed, GABAergic inhibition is modulated by many factors. Intracellular calcium ($[Ca^{2+}]_i$) is one of these factors. The elevation of $[Ca^{2+}]_i$ inhibits GABAergic transmission in hippocampal pyramidal neurones (Alger, 1991) and dentate gyrus granule cells (DGCs; Isokawa, 1998). One mechanism that might explain this phenomenon is the direct action of Ca^{2+} on the $GABA_A$ receptor ($GABA_AR$) that decreases its affinity by phosphorylation and/or dephosphorylation of various subunits (for review see Mody & Pearce, 2004). An alternative mechanism is the regulation of presynaptic GABA release by postsynaptic neurones. In this scheme, the depolarization-induced elevation of $[Ca^{2+}]_i$ in the postsynaptic cell initiates the synthesis and release of a retrograde messenger, an endogenous cannabinoid (eCB), that travels to presynaptic terminals and inhibits GABA release (depolarization-induced suppression of inhibition (DSI)). Understanding the $[Ca^{2+}]_i$-mediated alteration of $GABA_AR$ function is a very active area of research in hippocampal neurones, including DGCs. However, the susceptibility of DGCs to DSI is poorly understood.

Endogenous cannabinoids are natural ligands for the type I brain cannabinoid receptor (CB1R). Endogenous cannabinoids are produced as a result of the activation of G-protein-coupled receptors and/or the elevation of $[Ca^{2+}]_i$ (for review see Freund *et al.* 2003). Since the discovery of eCB as a retrograde messenger for the regulation of transmitter release in hippocampal pyramidal cells (Ohno-Shosaku *et al.* 2001; Wilson & Nicoll, 2001), similar roles have been discovered in other

 DOI: 10.1113/jphysiol.2005.094219

regions of the brain (Kreitzer & Regehr, 2001; Trettel & Levine, 2003). Retrograde eCB-mediated signalling facilitates the induction of long-term potentiation (LTP) (Carlson *et al.* 2002), and glutamatergic (Gerdeman *et al.* 2002), GABAergic (Chevaleyre & Castillo, 2003) and spike-timing (Sjostrom *et al.* 2003) long-term depression (LTD). The multiple ways that eCBs are involved in intercellular communication make eCBs important molecules at synapses. However, the role of eCBs in the dentate gyrus of the hippocampus is not clear, because DGCs have not been shown to utilize eCBs for the regulation of GABAergic transmission normally, but only after they experience seizures (Chen *et al.* 2003).

Degradative enzymes for eCBs and CB1 receptors are present throughout the dentate gyrus (Elphick & Egertova, 2001). In the dentate gyrus CB1Rs are strongly expressed at the cholecystokinin (CCK)-immunoreactive GABAergic axon terminals, and exogenous application of a synthetic CB1R agonist, WIN55,212-2 reduces inhibitory postsynaptic currents (IPSCs) in DGCs (Hajos *et al.* 2000). Together, the available evidence suggests that the $[Ca^{2+}]_i$-dependent depression of $GABA_A$R-mediated inhibition in DGCs could be explained by the eCB-mediated retrograde signalling. Thus, we tested if DGCs are capable of inducing DSI under normal conditions.

Methods

Sprague-Dawley rats (7–15 days, $n = 18$; and 3–4 weeks, $n = 11$) were deeply anaesthetized by halothane and decapitated. All experimental procedures and protocols were approved by the Institutional Animal Care and Use Committee of the University of Maryland School of Medicine. Brains were quickly removed and immersed in the ice-cold ACSF consisting of (mM): 124 NaCl, 3 KCl, 1.24 Na_2HPO_4, 2 $MgSO_4$, 2 $CaCl_2$, 26 $NaHCO_3$, 10 glucose (all from Sigma). Slices were cut 300 μm thick, and incubated in the oxygenated ACSF at $34 \pm 1^{\circ}$C for at least 1 h before experiments. All experiments were done at $34 \pm 1^{\circ}$C by warming the bath ACSF. We did not observe any difference in the data taken from the 4-week-old rat ($n = 11$) compared with 7–15 day rats ($n = 18$), so the data were pooled for analysis.

DGCs were visualized and voltage-clamped at –70 mV in the whole-cell configuration (Axopatch 200A, Axon Instruments). Patch pipettes were filled with (mM): 100 caesium methanesulphonate, 50 CsCl, 10 Hepes, 4 MgATP, 0.1 EGTA, and 5 QX-314 (all from Sigma), and had resistances of 3–5 MΩ in the bath. A field stimulating electrode (concentric bipolar stainless steel, 100 μm in diameter) was placed in the molecular layer to stimulate GABAergic axons directly (15 μA for 100 μs; S8800, Grass) in the presence of NBQX (10 μM) and DL-APV (100 μM)(both from Tocris Cookson) in order to produce monosynaptic IPSCs. In some experiments, carbachol (1–5 μM) was added to the ACSF in order to facilitate the generation of spontaneous IPSCs (sIPSCs) (Martin & Alger, 1999). Caffeine (20 mM, Sigma) was locally applied to DGC somata through a glass pipette (1–2 μm in diameter, 10–15 p.s.i. for 1.5 s) (Picospritzer, General Valve). Ryanodine (20 μM in a final concentration of 0.02% DMSO from 100 mM DMSO stock, Sigma), thapsigargin (2 μM, Sigma), SR141716A (1 μM at a final concentration of 0.01% DMSO from 10 mM stock, NIDA), CP55,942 (1 μM at a final concentration of 0.01% DMSO from 10 mM stock, Tocris), and WIN 55,212-2 (3 μM at a final concentration of 0.001% DMSO from 100 mM stock, Tocris) were bath-applied. In some experiments, ryanodine (50 μM) and ruthenium red (20 μM) were included in the patch pipette for intracellular application.

DSI was induced by applying a depolarizing voltage step (–70 to 0 mV for 0.5–3 s) through the recording pipette every 3–5 min. Frequencies of sIPSCs were calculated by determining the total number of sIPSCs occurring in time periods equal to the duration of DSI, and expressing this as sIPSCs s^{-1}. DSI of sIPSCs was calculated by the reduction in the frequencies. We grouped sIPSCs into the following four groups of amplitudes, i.e. <25 pA, 25–49 pA, 50–100 pA, and >100 pA. The basal frequency of sIPSCs was determined by dividing the total number of sIPSCs that appeared during a time period equal to the duration of DSI, but before the application of DSI-inducing voltage steps. Termination of DSI of sIPSCs was defined as the occurrence of more than three consecutive sIPSCs with amplitude greater than 100 pA within 10 s, because this corresponded to the average frequency of large (>100 pA) sIPSCs before the application of DSI-inducing voltage steps, i.e. basal level. DSI of evoked IPSCs (eIPSCs) was assessed by stimulating GABAergic terminals every 3 s, and by dividing the mean amplitude of five eIPSCs after the depolarizing step by the mean of five eIPSCs before the step.

For Ca^{2+} imaging, Oregon Green BAPTA-2 (200 μM) in cell-impermeant form (Molecular Probes) was dissolved in the intrapipette solution. Fluorescence signals were collected with a cooled CCD camera (Pixel-37, Photometrics) at a rate of 10 frames s^{-1}. Ten to 15 frames were acquired before the depolarizing voltage-step, and 150–250 frames were acquired after the step (Metafluor, Universal Imaging). Fura-2 100 μM was used in some neurones to monitor the stability of basal $[Ca^{2+}]_i$ levels during experiments, including ryanodine applications. Background subtraction was done in each frame using a region away from the neurones studied.

All data are reported as the mean ± S.E.M. Statistical significance was tested by ANOVA with repeated measures or a paired t test.

Results

DGCs are susceptible to DSI in a $[Ca^{+}]_i$-dependent manner

DGCs were selected from infra- and supra-pyramidal blades in the deep granule cell layer near the hilus, as well as from the superficial layer close to the molecular layer (Fig. 1*A*). DGCs are relatively sparsely distributed near the cresta at which proximal dendrites could be identified (Fig. 1*B*). The DSI-inducing depolarizing step was given every 3–5 min. A brief depolarization lasting from 1 to 3 s induced a transient cessation of sIPSCs (Fig. 1*D*–*F*). The DSI lasted from 17.98 s in response to 1 s depolarization, to 61.07 s after a 3 s depolarization, with a mean of 37.8 ± 4.79 s (mean ± S.E.M., $n = 21$). The longer depolarizing steps were more effective in generating longer-lasting DSI (Fig. 1*G*).

We found that the largest sIPSCs (>100 pA in amplitude) were most sensitive to DSI, while the smallest sIPSCs (<25 pA) were unaffected (Fig. 1*I* upper graph, also see Fig. 5*C* left graph). DSI was significant for all categories of sIPSCs >25 pA ($P < 0.001$), and its magnitude increased progressively as the sIPSCs became larger ($P < 0.01$). The mean amplitude of sIPSCs (<25 pA) was unaffected by the DSI-inducing depolarization (16.28 ± 0.22 pA before depolarization, and 15.99 ± 0.37 pA after depolarization; $P = 0.31$). Because the amplitude of mIPSCs falls in a similar range of <25 pA in DGCs (De Koninck & Mody, 1996), this result suggested that the reduction in the frequencies of the larger sIPSCs was unlikely to be due to postsynaptic factors.

Positive correlations between the duration of the depolarization and the magnitude of DSI suggested the induction of DSI in DGCs may be dependent on the increase of cytosolic calcium ($[Ca^{2+}]_i$), similar to what has been reported in CA1 pyramidal cells (Lenz & Alger, 1999; Wilson & Nicoll, 2001). In order to test this hypothesis, we included 10 mM BAPTA in the

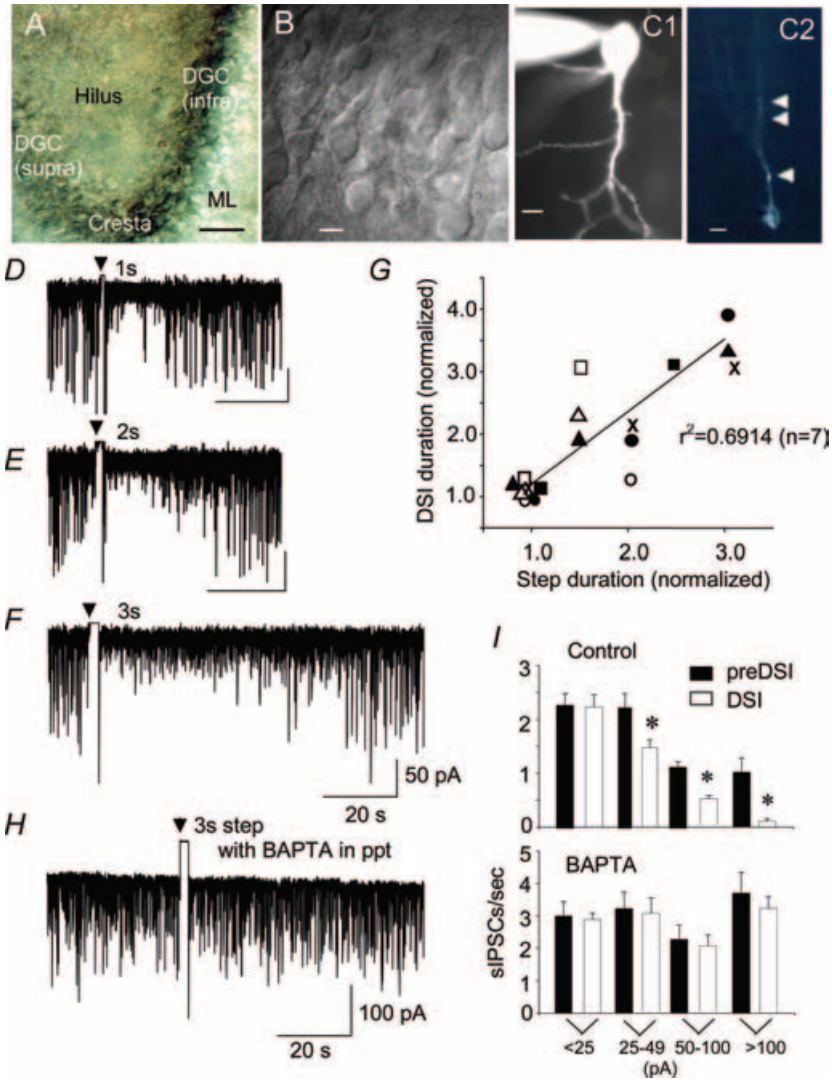

Figure 1. DGCs are capable of inducing DSI
A, dentate gyrus in hippocampal slice (calibration, 50 μm). ML, molecular layer. *B*, DGCs at cresta (calibration, 10 μm). *C*, fluorescent visualization of DGC with whole-cell recording. *C1* with Lucifer yellow (calibration, 5.5 μm), and *C2* with OGB488-2 (calibration, 10 μm). Arrowheads in *C2* indicate regional increases in fluorescence intensity. *D*–*F*, DSI with depolarizing voltage steps of 1, 2, or 3 s, respectively. *D*, *E* and *F* share the same calibration. *G*, correlation between the magnitude of depolarization and that of DSI. Data were normalized. Each cell has a different symbol. *H* and *I*, blockade of DSI by BAPTA (10 mM). Error bars indicate standard error of the mean (S.E.M.), and asterisks indicate $P < 0.01$.

intrapipette solution. BAPTA blocked the induction of DSI in response to the identical depolarizing voltage step (Fig. 1*H*, a representative example in $n = 4$, and Fig. 1*I* for group data). From this evidence we conclude that the DSI in DGCs requires a depolarization-induced elevation of $[Ca^{2+}]_i$.

DSI in DGC involves Ca^{+} release from ryanodine-sensitive stores

Ca^{2+} influx through voltage-dependent calcium channels is the initial source of the Ca^{2+} for the induction of DSI in the CA1 pyramidal cells (Lenz *et al.* 1998). We also found that Ca^{2+} from intracellular stores participated in the induction of DSI in the hippocampal CA1 cells of young animals (Isokawa & Alger, 2004). Hence Ca^{2+} from intracellular stores may contribute to the induction of DSI in DGCs. We therefore determined whether the DSI in DGCs was sensitive to thapsigargin, an endoplasmic reticulum Ca^{2+}-ATPase inhibitor, as well as to ryanodine and ruthenium red, ligands and antagonists for the ryanodine receptor Ca^{2+} release channel (RyR).

Caffeine sensitizes RyRs and induces Ca^{2+} release. Caffeine-sensitive Ca^{2+} stores have not been extensively characterized in DGCs. We first looked for the presence of caffeine-sensitive $[Ca^{2+}]_i$ signals in DGCs. A local brief puff application of caffeine (20 mM for 1.5 s) near the soma generated a multimodal Ca^{2+} response (Fig. 2*A*). The early response was rapid and created a large sharp peak. The late response developed slowly after the completion of the early response, and formed a smaller but broader secondary peak. The late response lasted over 15 s. We observed similar biphasic Ca^{2+} responses to caffeine in five additional DGCs with calcium green 5N and Fluo4-FF. Bath application of ryanodine (20 μM for 15 min) blocked the early peak and also substantially reduced the late peak of the caffeine-induced $[Ca^{2+}]_i$ signals. From these data, we confirm that DGCs do have caffeine- and ryanodine-sensitive Ca^{2+}-stores.

Although this experiment showed that Ca^{2+} could be released from intracellular Ca^{2+} stores by caffeine, it was not clear if this source of Ca^{2+} could play a role in DSI. Hence, we next tested the effect of ryanodine on the depolarizing step-induced $[Ca^{2+}]_i$ signals. A depolarizing voltage step produced a transient increase in $[Ca^{2+}]_i$ that peaked at the end of the depolarization step. The subsequent application of ryanodine in the bath reduced the peak amplitude of this $[Ca^{2+}]_i$ increase. The peak latency of the $[Ca^{2+}]_i$ response was unaffected (Fig. 2*B*). This result suggests that the activation of RyRs probably occurs immediately after the depolarization is initiated, and the release of Ca^{2+} from RyRs constitutes an

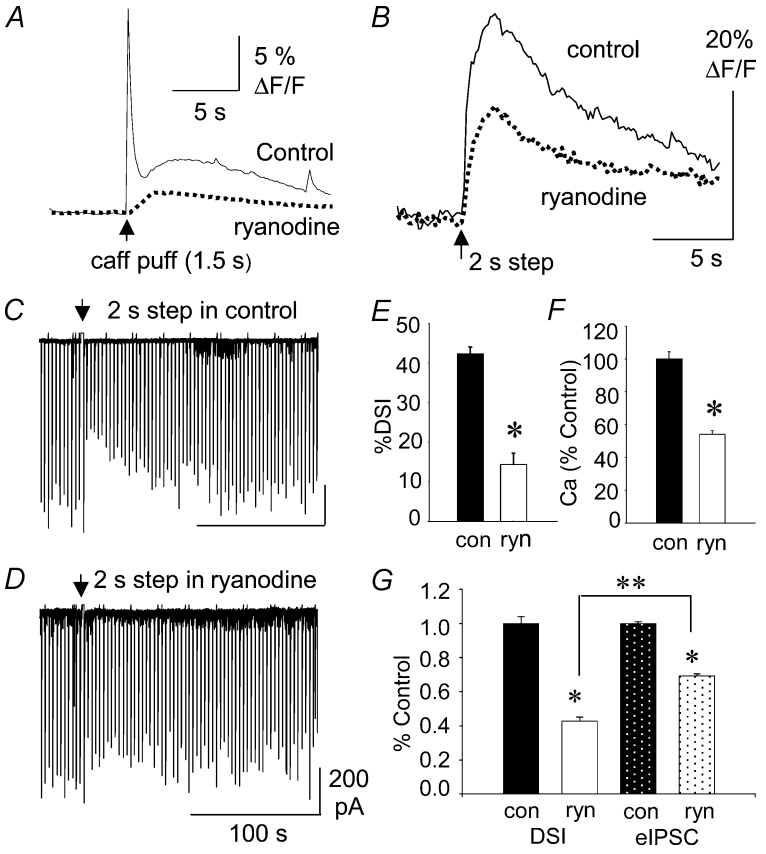

Figure 2. DSI in DGCs involves Ca^{2+} release from intracellular stores
A, caffeine-induced $[Ca^{2+}]_i$ increase in control (continuous line) and in the same cell after bath application of ryanodine (20 μM bath, broken line); $\Delta F/F$ is a relative change in the fluoresence intensity. *B*, depolarization-induced $[Ca^{2+}]_i$ increase in control (continuous line) and in the same cell after bath application of ryanodine (broken line). *C*, DSI recorded simultaneously with the $[Ca^{2+}]_i$ signals shown in *B*. *D*, blockade of DSI by ryanodine accompanied by the reduction in $[Ca^{2+}]_i$ signals shown in *B*. *C* and *D* share the same calibration. *E*, reduction in the magnitude of DSI by ryanodine (E, $n = 6$). *F*, reduction in the depolarization-induced $[Ca^{2+}]_i$ signals by ryanodine (ryn). *G*, reduction in the magnitude of DSI exceeded the reduction of eIPSC amplitude in ryanodine. Data were normalized ($^{*}P < 0.0001$; $^{**}P < 0.001$) and error bars show S.E.M.

appreciable component of the depolarization-induced increase of $[Ca^{2+}]_i$.

We next examined the effect of ryanodine on DSI while simultaneously imaging $[Ca^{2+}]_i$ signals from the same neurones. As shown in Fig. 2*C*, a 2 s depolarization in control ACSF induced DSI that typically lasted over a minute and had an average magnitude of over 40%. Subsequent application of ryanodine (20 μM) reduced the magnitude of DSI in response to the identical depolarization (Figs 2*D* and *E*, $P < 0.0003$, $n = 6$, paired *t* test). $[Ca^{2+}]_i$ signals recorded with DSI were also reduced to $54.2 \pm 2.09\%$ of control in these cells ($P < 0.002$ in Fig. 2*F*).

DSI could appear reduced if ryanodine reduced DSI-susceptible eIPSCs even if the actual DSI process were not affected. Therefore, we examined the basal amplitude of eIPSCs. The mean amplitude of eIPSCs before the depolarizing step was 557.46 ± 5.62 pA in control, and 391.58 ± 19.78 pA in ryanodine. The reduction in the basal eIPSC amplitude in ryanodine was significant ($P < 0.001$), suggesting that ryanodine might have affected RyRs in the presynaptic terminals during GABA release, as such effects have been reported in the cerebellar Purkinje cells (Galante & Marty, 2003). Thus, we compared the relative changes in the magnitude of DSI and the basal eIPSC amplitude in ryanodine. As shown in Fig. 2*G*, DSI was reduced by 53.6% in ryanodine ($P < 0.0001$), while the basal amplitude of eIPSC before the DSI-inducing depolarization was reduced by only 29.8% in ryanodine ($P < 0.0001$). The greater reduction in the magnitude of DSI than the reduction in the amplitude of basal eIPSCs ($P < 0.001$) suggested that the decrease in the magnitude of DSI was not solely due to the presynaptic action of ryanodine on the GABA-release mechanism.

In order to further test this interpretation, we applied ryanodine intracellularly. Ryanodine is cell permeant, so that intracellularly delivered ryanodine can diffuse out from the cell, and may affect presynaptic terminals. However, the intracellular application of ryanodine can create a local high concentration of ryanodine within the cell applied, while the extracellular concentration of ryanodine can be kept negligible by an infinitely larger volume of bath ACSF compared with the volume of cytosol. We also used a cell-impermeant form of RyR antagonist, ruthenium red (RR), in our patch pipettes in order to block the RyR Ca^{2+} channel during the induction of DSI. Ryanodine or RR applied through the pipette will diffuse into the cytosol as soon as the whole cell configuration is established, thus they could start exerting their effects on RyR at any given time after the break-in. In order to properly assess the effects of ryanodine and RR on the induction of DSI, it was important to ensure that the DGCs that we sampled with ryanodine/RR-containing pipettes were capable of producing DSI. We applied a depolarizing voltage step of 3 s within 3 min of break-in. Only the cells that showed DSI were used for further recordings and analysis. As demonstrated in Fig. 3, DGCs showed DSI 3 min after the break-in even if ryanodine or RR was included in the recording pipette. Ca^{2+} transients were also recorded as relative increases in response to the DSI-inducing depolarizing voltage steps. At 24 min after the break-in, DSI was largely inhibited, and the peak amplitudes of the Ca^{2+} transients were also decreased.

We conducted a time course study with the pipette solution that did not contain ryanodine or RR, as a control for the intracellular application of ryanodine or RR. In this experiment, the recording and imaging lasted for the same duration as those with the ryanodine or RR application. As shown in Fig. 3*C*, DSI lasted over 40 min without any change in the magnitude in the control group, showing that the reduction in DSI with intracellular application of ryanodine or RR was due to their effect on RyR. The differences between DSI in the ryanodine- or RR-treated cells and control cells at 40 min after break-in were significant ($P < 0.005$ for ryanodine, $P < 0.01$ for RR). The Ca^{2+} peak was also reduced to $47.3\% \pm 8.93$ of the original with RR ($P < 0.05$), and to $27.1\% \pm 3.33$ of the original with ryanodine ($P < 0.005$) by 40 min after the break-in. These findings suggested that the amplification of $[Ca^{2+}]_i$ signals during depolarization through the release of Ca^{2+} from RyRs was involved in the induction of DSI in DGCs.

Finally, we tested the effect of depleting the Ca^{2+} stores with thapsigargin (TG) on the induction of DSI. As summarized in Fig. 4, TG inhibited the major portion of DSI in eIPSCs and sIPSCs (Fig. 4*A* and *C*). The TG-sensitive reduction of DSI was significant only for sIPSCs that were greater than 50 pA. The Ca^{2+} transients caused by the DSI-inducing depolarizing step were also reduced (Figs 4*B* and *D*). These findings with TG confirmed our previous data with ryanodine and RR, that a Ca^{2+} release from intracellular stores plays an indispensable role for determining the magnitude of DSI in DGCs.

DSI in DGC is CB1R dependent

We tested whether the DSI in DGC is mediated by eCBs and CB1R, as reported in CA1 hippocampus (Wilson & Nicoll, 2001). sIPSCs were recorded, and their amplitudes were categorized into four groups as defined in Fig. 1. A depolarizing voltage step of 500 ms was delivered eight times at 1 Hz (50% duty cycle). This induced DSI of sIPSCs greater than 25 pA in control ACSF (Fig. 3*A* and *C*); sIPSCs >100 pA were most sensitive to DSI. Subsequently, the CB1R antagonist, SR141716A (1–2 μM) was bath-applied. After 15–20 min of bath application, the identical voltage steps were delivered. In the presence

of SR141716A, these voltage steps failed to generate DSI (Fig. 3*B* and *D*). However, SR141716A did not change basal frequencies of sIPSCs of any amplitude.

We next examined the effect of CB1R agonists on DSI by applying CP55,942 and WIN55,212-2 in the bath ACSF. Both CP55,942 and WIN55,212-2 will activate CB1R and thus inhibit the release of GABA from CB1R-bearing axon terminals, independently of postsynaptic depolarization. In the presence of these agonists, the effect of eCBs that are produced by depolarization, i.e. DSI, is predicted to be absent. Indeed, DSI of both sIPSCs and eIPSCs disappeared when these agonists were added to the bath (Fig. 5*D*). This disappearance of DSI reflected the mimicry of DSI, not blockade, because the agonists reduced the amplitude of eIPSCs and sIPSCs to the same extent as DSI. There were no differences between the amplitude of eIPSCs during DSI in the absence of CB1R agonists, and the amplitude of eIPSCs in the presence of these agonists (right graph in Fig. 5*D*). Similarly, there were no differences in the frequencies of sIPSCs before and after the DSI-inducing depolarizing steps in the presence of the CB1R agonist (Fig. 5*D* left two traces). The mean frequency for sIPSCs <25 pA was $1.82 \pm 0.1\ s^{-1}$ before the step and $1.93 \pm 0.39\ s^{-1}$ after the step. For sIPSCs of 25–49 pA, it was $1.17 \pm 0.21\ s^{-1}$ before the step and $0.90 \pm 0.01\ s^{-1}$ after the step, and for sIPSCs of 50–100 pA, it was $0.48 \pm 0.06\ s^{-1}$ before the step and $0.39 \pm 0.09\ s^{-1}$ after the step. We did not observe any sIPSCs >100 pA in the presence of CP55,942, which confirmed our observations that the largest sIPSCs were most sensitive to DSI. These findings strongly suggest that eCBs mediate DSI in DGC.

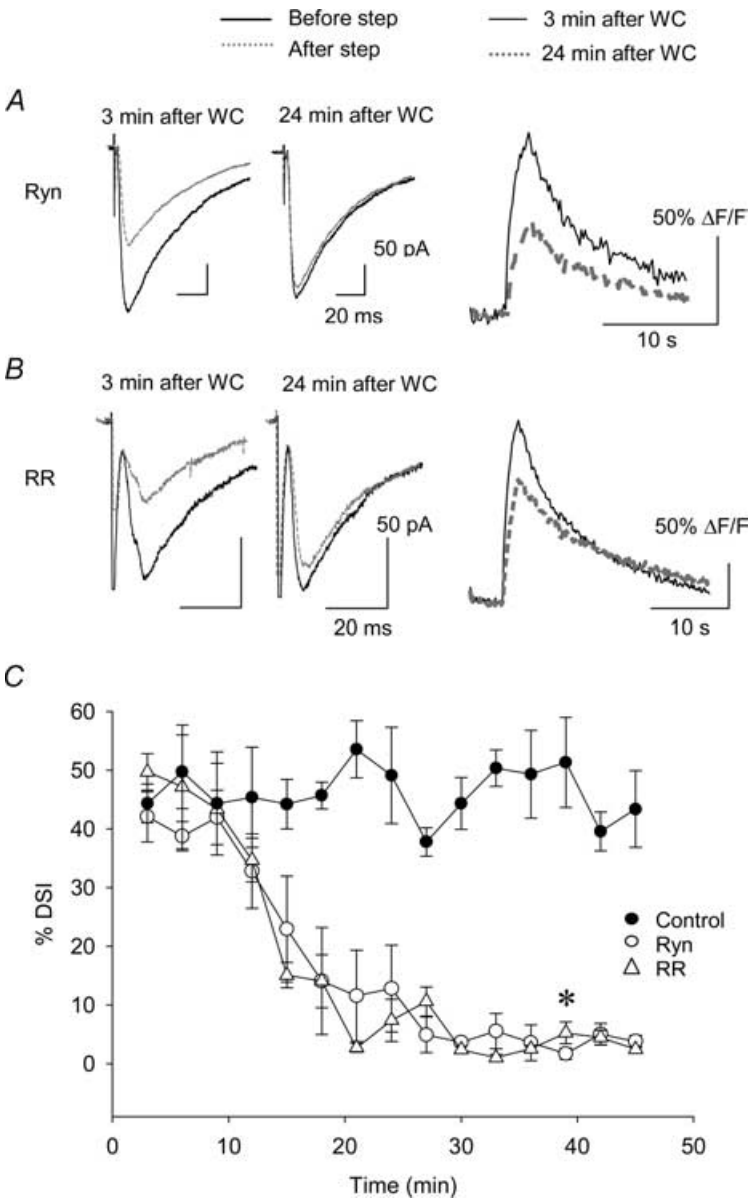

Figure 3. Intracellular application of ryanodine or ruthenium red inhibits the induction of DSI
DSI was recorded every 3 min after the establishment of whole-cell recording. DSI was apparent 3 min after the break-in with intrapipette application of ryanodine (Ryn) (*A*) or ruthenium red (RR) (*B*). However, by 24 min, DSI was reduced by these compounds. Depolarization-induced Ca^{2+} increase was also reduced by ryanodine (right plot in *A*) and ruthenium red (right plot in *B*). *C*, time-dependent decrease in the magnitude of DSI with intracellular application of ryanodine (Ryn) or ruthenium red (RR) ($P < 0.01$ at 40 min after the break-in). Error bars show S.E.M.

Discussion

The present study shows: (1) DGCs are susceptible to DSI; (2) DSI in DGC is $[Ca^{2+}]_i$ dependent, and involves the RyR-mediated Ca^{2+} release; and (3) eCBs act as retrograde messengers in the dentate gyrus.

This report is the first to demonstrate that DGCs can normally show DSI. Our findings are somewhat at odds with a previous report that DGCs only showed DSI after experimental febrile seizures (Chen *et al.* 2003). The seizures induced the appearance of DSI, and increased the number of CB1Rs, without obvious changes in the levels of eCBs or eCB metabolism. Technical differences between our recording conditions and those of Chen *et al.* may explain the apparent discrepancy. We do agree with Chen *et al.* (2003) that the CB1 antagonist, SR141716A had no effect on IPSCs in DGCs in normal conditions, implying that eCBs do not appear to exert a tonic influence in DGCs.

We found that Ca^{2+} release from caffeine/ryanodine-sensitive stores plays a critical role in the induction of DSI in DGCs. Our observation that ryanodine and ruthenium red reduced the depolarization-induced $[Ca^{2+}]_i$ increase at the earliest time point that we can measure after the onset of the voltage-step suggests there is close coupling between calcium influx through voltage-gated calcium channels (VGCCs) and RyR-mediated Ca^{2+} release. In the CA1 pyramidal cell, high-threshold Ca^{2+} channels, N-type and L-type, are the likely sources of calcium influx for the induction of DSI (Lenz *et al.* 1998). Both N-type (Akita & Kuba, 2000) and L-type channels (Chavis *et al.* 1996) have tight functional coupling with RyRs in neurones. P/Q-type VGCC may also couple functionally with RyRs in the dendrites and spines of cerebellar Purkinje cells (Hartmann & Konnerth, 2005). Future work will be required to determine the mechanisms of RyR activation in DGCs. The contribution of RyR-mediated Ca^{2+} release to the eCB production during DSI that we found in DGCs may be similar to the role of RyR in eCB production in the depolarization-induced suppression of excitation in

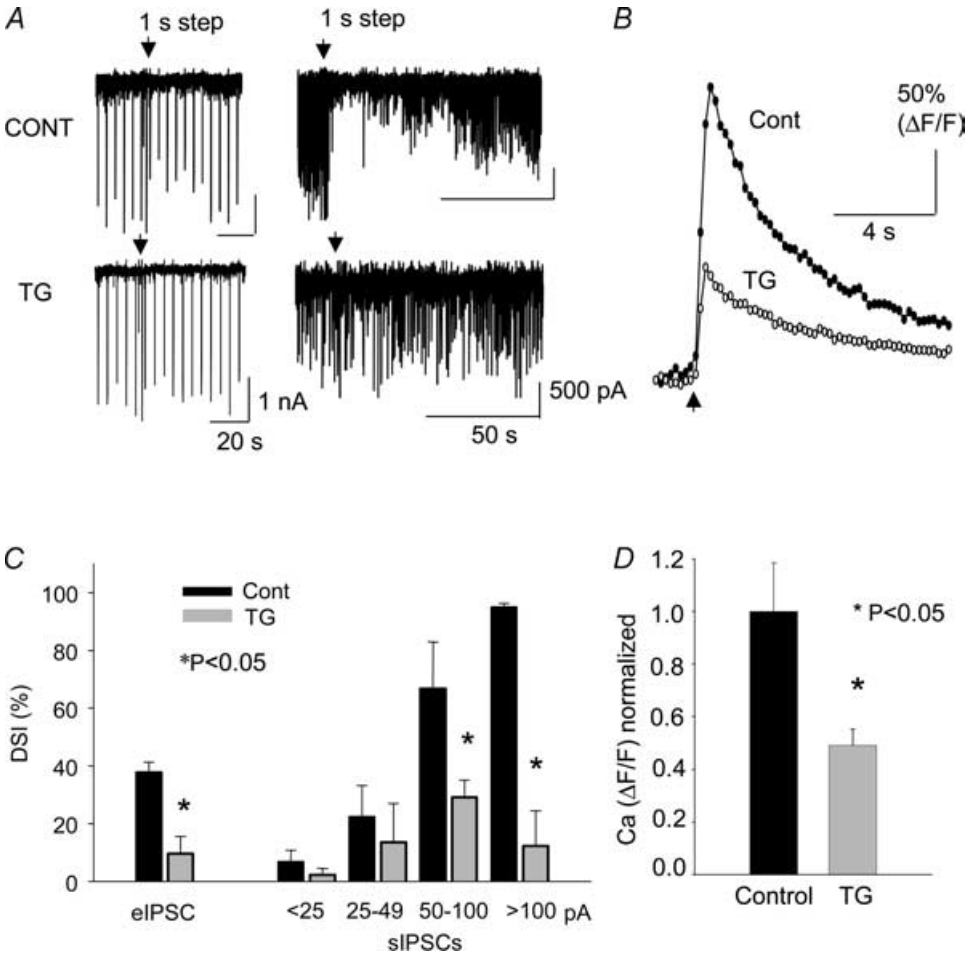

Figure 4. Depletion of Ca^{2+} stores downregulates the magnitude of DSI
A, thapsigargin (TG, 2 μM in the bath) reduced the magnitude of sIPSC/eIPSC DSI. *B*, Ca^{2+} transients, induced by the DSI-inducing depolarizing steps, were also reduced by TG (*D* for group data). *C*, the reduction in DSI by TG was significant with sIPSCs of 50 pA in amplitude or greater. Error bars show S.E.M.

the ventral tegmental area (Melis *et al.* 2004), and in LTD in the nucleus accumbens (Robbe *et al.* 2002). Thus, our data suggest that RyR may play a fundamental role in eCB synthesis across different cell types.

We used two forms of depolarization to induce DSI: a single long-lasting depolarizing step of 1–3 s, or a series of short (500 ms) repetitive depolarizations. The latter was sometimes more effective in inducing DSI for the first time in DGCs. A similar protocol for the induction of DSI with repetitive short depolarization was used for the cerebellar Purkinje cell (Diana & Marty, 2003). Both DGCs and Purkinje cells have high $[Ca^{2+}]_i$-buffering capacity, because they have a high concentration of calbindin D-28k, a calcium-binding protein, compared to CA1 pyramidal cells, which have a low $[Ca^{2+}]_i$-buffering capacity (Baimbridge *et al.* 1992). The dominant isoform of RyRs in DGCs and Purkinje cells is RyR1, in contrast to the CA1 pyramidal cells, in which the dominant

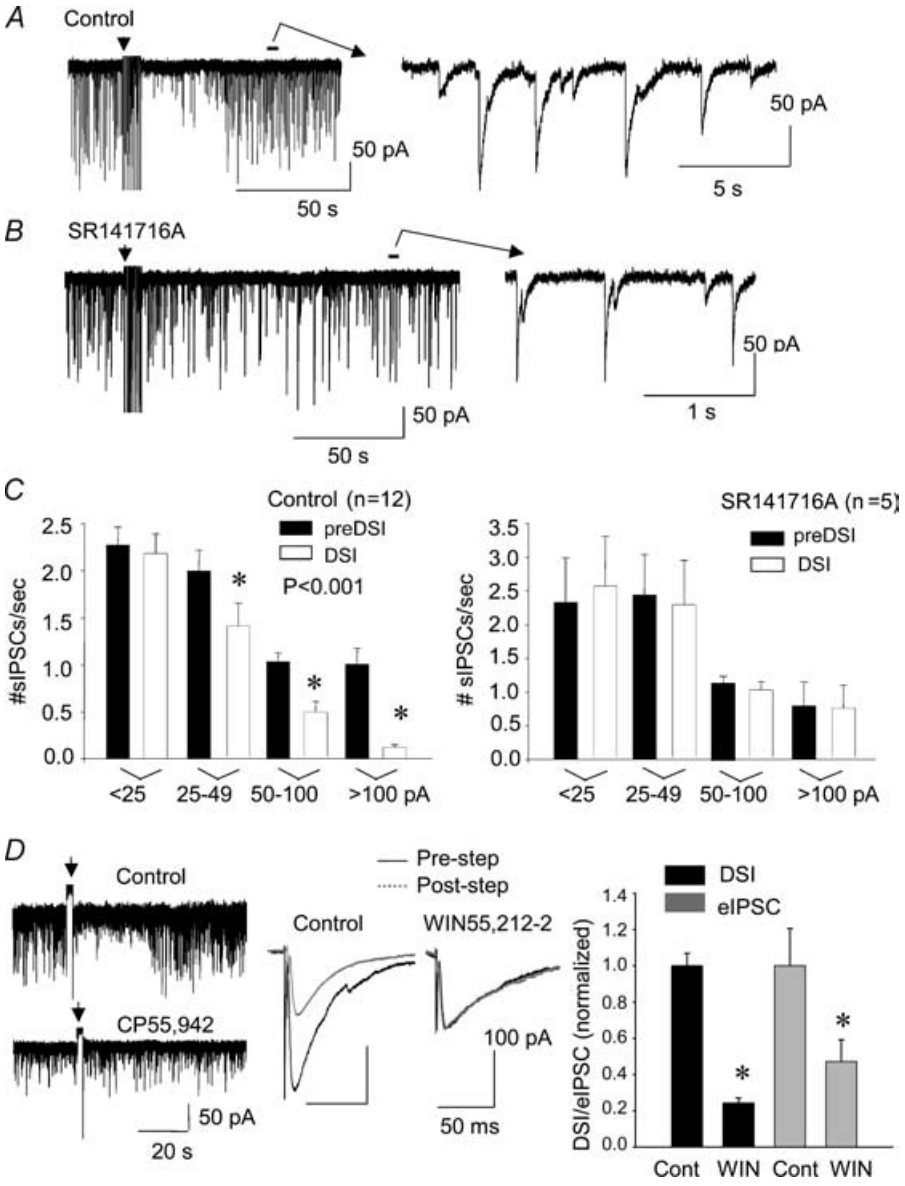

Figure 5. DSI in DGC is CB1R dependent

A, DSI in control. *B*, blockade of DSI by SR141716A. Right traces in *A* and *B* are examples of sIPSCs taken from the part indicated by horizontal bars. Amplitude calibrations in *A* and *B* are all 50 pA. *C*, DSI affected sIPSCs with amplitudes greater than 25 pA (*$P < 0.001$, left graph), and was blocked by SR141716A (differences between bars not significant, $0.319 < P < 0.794$; right graph). *D*, mimicry of DSI by the CB1R agonists, CP55,942 (left traces, sIPSCs) and WIN 55,212-2 (middle traces, eIPSCs), prevented further IPSC reduction by DSI. The reductions in the amplitudes of eIPSCs by depolarization and by WIN 55,212-2 were both significant (*$P < 0.05$); however, the magnitude of the reduction by depolarization and WIN 55,212-2 was not different (right graph). Error bars are S.E.M.

isoform is RyR2 (Mori *et al.* 2000). The effectiveness of the linkage between the depolarization-induced $[Ca^{2+}]_i$ elevation to the activation of different isoforms of RyRs might be reflected in the mode of depolarization employed (Fill & Copello, 2002).

In conclusion, DSI may be normally induced in DGCs as a means of regulating GABAergic inhibition in the dentate gyrus. The dentate gyrus is a gateway for the incoming cortical inputs to the hippocampus, and our study paves the way for future investigations of eCB-mediated mechanisms of learning and plasticity in DGCs.

References

Akita T & Kuba K (2000). Functional triads consisting of ryanodine receptors, Ca^{2+} channels, and Ca^{2+}-activated K+ channels in bullfrog sympathetic neurons. Plastic modulation of action potential. *J Gen Physiol* **116**, 697–720.

Alger BE (1991). Gating of GABAergic inhibition in hippocampal pyramidal cells. Activity-driven CNS changes in learning and development. *Ann N Y Acad Sci* **627**, 249–263.

Alger BE (2002). Retrograde signaling in the regulation of synaptic transmission: focus on endocannabinoids. *Prog Neurobiol* **68**, 247–286.

Baimbridge KG, Celio MR & Rogers JH (1992). Calcium-binding proteins in the nervous system. *Trends Neurosci* **15**, 303–308.

Carlson G, Wang Y & Alger BE (2002). Endocannabinoids facilitate the induction of LTP in the hippocampus. *Nature Neurosci* **5**, 723–724.

Chavis P, Fagni L, Lansman JB & Bockaert J (1996). Functional coupling between ryanodine receptors and L-type calcium channels in neurons. *Nature* **382**, 719–722.

Chen K, Ratzliff A, Hilgenberg L, Gulyas A, Freund TF, Smith M, Dinh TP, Piomelli D, Mackie K & Soltesz I (2003). Long-term plasticity of endocannabinoid signaling induced by developmental febrile seizures. *Neuron* **39**, 599–611.

Chevaleyre V & Castillo PE (2003). Heterosynaptic LTD of hippocampal GABAergic synapses. A novel role of endocannabinoids in regulating excitability. *Neuron* **38**, 461–472.

De Koninck Y & Mody I (1996). The effects of raising intracellular calcium on synaptic $GABA_A$ receptor-channels. *Neuropharmacology* **35**, 1365–1374.

Diana MA & Marty A (2003). Chartacterization of depolarization-induced suppression of inhibition using paired interneuron–Purkinje cell recordings. *J Neurosci* **23**, 5906–5918.

Elphick MR & Egertova M (2001). The neurobiology and evolution of cannabinoid signaling. *Phil Trans R Soc Lond B* **356**, 381–408.

Fill M & Copello JA (2002). Ryanodine receptor calcium release channels. *Physiol Rev* **82**, 893–922.

Freund T, Katona I & Piomelli D (2003). Role of endogenous cannabinoids in synaptic signaling. *Physiol Rev* **83**, 1017–1066.

Galante M & Marty A (2003). Presynaptic ryanodine-sensitive calcium stores contribute to evoked neurotransmitter release at the basket cell-Purkinje cell synapse. *J Neurosci* **23**, 11229–11234.

Gerdeman GL, Ronesi J & Lovinger DM (2002). Postsynaptic endocannabinoid release is critical to long-term depression in the striatum. *Nature Neurosci* **5**, 446–451.

Hajos N, Katona I, Naiem SS, Mackie K, Ledent C, Mody I & Freund TF (2000). Cannabinoids inhibit hippocampal GABAergic transmission and network oscillations. *Eur J Neurosci* **12**, 3239–3249.

Hartmann J & Konnerth A (2005). Determinants of postsynaptic Ca^{2+} signaling in Purkinje neurons. *Cell Calcium* **37**, 459–466.

Isokawa M (1998). Modulation of $GABA_A$ receptor-mediated inhibition by postsynapic calcium in epileptic hippocampal neurons. *Brain Res* **810**, 241–250.

Isokawa M & Alger BE (2004). Ryanodine-sensitive calcium signals in the release of endocannabinoids in the hippocampus. *Program No. 623.16 2004 Abstract Viewer/Itinerary Planner*. Washington, DC: Society for Neuroscience, 2004. Online.

Kreitzer AC & Regehr WG (2001). Retrograde inhibition of presynaptic calcium influx by endogenous cannabinoids at excitatory synapses onto Purkinje cells. *Neuron* **29**, 717–727.

Lavenex P & Amaral D (2000). Hippocampal–neocortical interaction: a hierarchy of associativity. *Hippocampus* **10**, 420–430.

Lenz RA & Alger BE (1999). Calcium dependence of depolarization-induced suppression of inhibition in rat hippocampal CA1 pyramidal neurons. *J Physiol* **521**, 147–157.

Lenz RA, Wagner JJ & Alger BE (1998). N- and L-type calcium channel involvement in depolarization-induced suppression of inhibition in rat hippocampal CA1 cells. *J Physiol* **512**, 61–73.

Martin LA & Alger BE (1999). Muscarinic facilitation of the occurrence of depolarization-induced suppression of inhibition in rat hippocampus. *Neuroscience* **92**, 61–71.

Melis M, Perra S, Muntoni AL, Pillolla G, Lutz B, Marsicano G, Di Marzo V, Gessa GL & Pistis M (2004). Prefrontal cortex stimulation induces 2-arachidonoyl-glycerol-mediated suppression of excitation in dopamine neurons. *J Neurosci* **24**, 10707–10715.

Mody I & Pearce RA (2004). Diversity of inhibitory neurotransmission through $GABA_A$ receptors. *Trends Neurosci* **27**, 569–575.

Mori F, Fukaya M, Abe H, Wakabayashi K & Watanabe M (2000). Developmental changes in expression of the three ryanodine receptor mRNA in the mouse brain. *Neurosci Lett* **285**, 57–60.

Ohno-Shosaku T, Maejima T & Kano M (2001). Endogenous cannabinoids mediate retrograde signals from depolarized postsynaptic neurons to presynaptic terminals. *Neuron* **29**, 729–738.

Robbe D, Kopf M, Remaury A, Bockaert J & Manzoni OJ (2002). Endogenous cannabinoids mediate long-term synaptic depression in the nucleus accumbens. *Proc Natl Acad Sci U S A* **99**, 8384–8388.

Sjostrom PJ, Turrigiano GG & Nelson SB (2003). Neocortical LTD via coincident activation of presynaptic NMDA and cannabinoid receptors. *Neuron* **39**, 641–654.

Trettel J & Levine ES (2003). Endocannbinoids mediate rapid retrograde signaling at interneuron–pyramidal neuron synapses of the neocortex. *J Neurophysiol* **89**, 2334–2338.

Wilson RI & Nicoll RA (2001). Endogenous cannabinoids mediate retrograde signalling at hippocampal synapses. *Nature* **410**, 588–592.

Acknowledgements

This work is supported by NIH grants NS31180, DA014625 and NS30219, University of Maryland Other Tobacco Related Disease grant, and Bressler Research Award.

Author's present address

M. Isokawa: Department of Biological Sciences, The University of Texas at Brownsville, 80 Fort Brown, Brownsville, TX 78520, USA.